1-Butene Oligomerization in Brönsted Acidic Zeolites: Mechanistic Insights from Low-Temperature in Situ FTIR Spectroscopy

Morten Bjørgen,[†] Karl-Petter Lillerud,[†] Unni Olsbye,[†] Silvia Bordiga,[‡,§] and Adriano Zecchina*[,‡,§]

Department of Chemistry, University of Oslo, P.O. Box 1033, N-0315 Oslo, Norway, Dipartimento di Chimica I.F.M., Università di Torino, via Pietro Giuria 7, I-10125 Torino, Italy, and INSTM UdR di Torino and INFM UdR di Torino, Università

Received: December 10, 2003; In Final Form: March 5, 2004

1-Butene has been reacted over H-beta, H-MCM-22, and H-mordenite, starting at 77 or 300 K. The systems were followed in situ by FTIR spectroscopy. At 300 K, 1-butene oligomerized instantaneously, and mechanistic information about the initial interactions between the active sites and the olefin and the subsequent chain growth was not inferable. Mechanistic details about the oligomerization reactions were provided by adsorbing 1-butene at 77 K and slowly heating the catalyst wafers to 300 K, while collecting spectra continuously. 1-Butene forms transient H-bonded precursors with the acidic sites of the zeolites prior to oligomerization. The strength of the H-bonded precursors formed into the three frameworks seems to be very similar, suggesting equal acidities of the Brönsted sites. These adducts were observable only at the lowest temperatures, and their concentration soon reached a maximum when the temperature was raised and vanished as the oligomerization reactions proceeded. Among the three zeolite samples, the oligomeric chains appear to grow most extensively in the three-dimensional beta zeolite.

1. Introduction

Acid-catalyzed oligomerization of alkenes to a variety of higher molecular weight homologues is an extensively studied area of petroleum chemistry. The technology for light alkene utilization via acid catalysis extends back to the 1930s with the commercialization of a process developed by UOP to convert propene and butene to dimers and trimers with phosphoric acid as catalysts.[1−5] The purpose of the process was to upgrade byproduct cracking gases to higher boiling products suitable for, for example, gasoline. Since then, a variety of processes and catalysts have been developed and commercialized. Today, oligomerization of light alkenes represents an important route for production of high-octane, environmentally friendly liquid fuels.

Among the various alkene oligomerization processes, dimerization of butene has received a major part of the attention lately.[6−8] Since the standard high-octane oxygenate blending component, methyl *tert*-butyl ether (MTBE), is about to be phased out, there is a need for alternative octane-enhancing gasoline components. The most attractive alternatives seem to be hydrogenated branched butene dimers, i.e., branched octanes. In particular, isooctane (2,2,4-trimethylpentane) appears to be a promising oxygen- and sulfur-free alternative to MTBE.

An advantage of zeolite-based olefin oligomerization routes is that only minimal olefin feed purification is required. Compared to the commonly employed "solid phosphoric acid catalyst" (i.e., phosphoric acid impregnated on a carrier of kieselguhr), zeolitic systems also have the advantages of being stable over a wide temperature range and, thus, being regenerable. Furthermore, zeolites are naturally occurring minerals that are not environmentally harmful. A disadvantage with zeolites is, however, the rather rapid catalyst deactivation they suffer from. Details about the olefin reactions occurring within the zeolite pores and the influence of parameters such as acid site density, acid site strength, and pore geometry on, for example, catalyst lifetime and product selectivities still remain unrevealed. A deeper understanding of these details will be of importance in the development of more efficient zeolite-based catalysts.

Among zeolite-based catalysts, wide pore structures appear to be the best suited systems for butene oligomerization since they allow highly branched hydrocarbons (i.e., hydrocarbons having a high octane number) to leave the channel system. In this work we report, from in situ measurements, the IR spectra of the transient H-bonded species and the oligomers formed upon 1-butene adsorption on H-beta, H-MCM-22, and H-mordenite.

2. Experimental Section

Three wide pore zeolite samples of protonic form have been employed in this study: H-beta (Si/Al = 12), H-MCM-22 (Si/Al = 11), and H-mordenite (Si/Al = 22). Elemental compositions were determined by ICP-AES. The samples of H-mordenite and H-beta were commercially available from Süd Chemie and P.Q. Zeolites B.V., respectively. H-MCM-22 was synthesized in our laboratory according to the procedure reported by Güray et al.[9]

The zeolite samples were compressed into self-supporting wafers and mounted in a gold envelope sample holder. Before adsorption of 1-butene, the samples were outgassed in situ for 1 h at 400 °C under high vacuum to remove water and other

* To whom correspondence should be addressed. Phone: +39-011-6707860. Fax: +39-011-6707855. E-mail: adriano.zecchina@unito.it.
[†] University of Oslo.
[‡] Università di Torino.
[§] INSTM UdR di Torino and INFM UdR di Torino.

10.1021/jp0377836 CCC: $27.50
Published on Web 05/18/2004

adsorbed impurities. 1-Butene, previously purified by repeated freeze−pump−thaw cycles, was dosed from a vacuum line permanently attached to the IR cell. The reactions were followed after adsorbing 5 Torr 1-butene on the zeolites at room temperature or at liquid nitrogen temperature. When starting at liquid nitrogen temperature, the IR cell was subsequently equilibrated thermally with the surroundings while spectra were collected continuously every 5.4 s. Apart from enhancing the reaction and diffusion rates, the rising temperature will also increase the partial pressure of 1-butene, as the starting temperature is slightly below the freezing point of 1-butene. The IR spectra were obtained in transmission mode on a Bruker IFS 66 FTIR spectrometer, equipped with a cryogenic MCT detector, at 4 cm^{-1} resolution. To give relatively fast acquisitions, only eight interferograms were recorded for each spectrum.

3. Results and Discussion

3.1. Structural Characteristics of H-Beta, H-MCM-22, and H-Mordenite. The beta zeolite is a highly intergrown hybrid of three polymorphs, A, B, and C.[10,11] All three polymorphs have a three-dimensional 12-ring channel system. The structures are internally ordered, but the stacking results in disorder along the [001] direction. For all the modifications, two channel systems are linear and topologically identical. They are mutually orthogonal and perpendicular to [001]. These two sets of channels intersect and form a third channel system that is sinusoidal and parallel to the *c*-axis. Polymorph A has a tetragonal framework, and the polymorphs B and C both have a monoclinic symmetry. The linear channels of polymorph A have the dimensions 6.6 × 7.7 Å, and the tortuous channel is smaller, 5.6 × 5.6 Å.[12]

MCM-22 is a high-silica zeolite having a rather peculiar framework structure comprised of two independent pore systems, both accessible through 10-membered rings. One of them is composed of two-dimensional sinusoidal 10-membered ring channels (apertures 5.5 × 4.0 and 5.1 × 4.1 Å),[12] and the other consists of large super cages with inner diameter 7.1 Å delimited by 12-membered rings. The unusual porous network of MCM-22 has characteristics between those of large- and medium-pore zeolites, and MCM-22 often shows properties similar to those of 12-ring zeolites.[13] As revealed by Lawton et al., external zeolitic pockets (each of those is half of a supercage) cover the surface of the crystals and may influence the catalytic properties of this material.[14]

The mordenite structure has 12- and eight-membered ring channels that run parallel to the *c*-axis. These systems are connected by eight-ring channels parallel to the *b*-axis. Typical channel dimensions are 6.5 × 7.0 and 5.7 × 2.6 Å for the 12- and eight-membered rings, respectively.[12] The access for most molecules to the interconnecting eight-ring channels is sterically hindered, and the channel system is thus one-dimensional in practice.

The acidic properties of the zeolite samples were probed by FTIR and CO at 77 K and are described in the Supporting Information.

3.2. Expected Reaction Route for 1-Butene Oligomerization. The 1-butene oligomerization reaction can generally be considered to be composed of three steps: initiation, propagation, and termination. This reaction sequence is illustrated in Scheme 1. The respective rates of propagation and termination are represented by the rate constants k_p and k_t in Scheme 1a. The reaction is suggested to be initiated by an interaction between the acidic sites of the zeolite and the π-electrons of 1-butene, resulting in a H-bonded precursor (Scheme 1a). The nature of the reaction intermediates may range from such a weakly bound, partly protonated species to a fully protonated species that is either bound covalently to the lattice as an alkoxy group or bound ionically to the lattice as a carbenium ion. Carbenium ions formed from species having a proton affinity as low as the one measured for 1-butene have not been observed in zeolites. In Scheme 1, a formal representation of reaction intermediates as alkoxy species has been adopted. The termination step, the rate of which is represented by the rate constant k_t in Scheme 1a, may be considered to be a simple desorption process. Desorption may lead to the formation of any alkene isomer, such as *cis*-2-, *trans*-2-, or iso-butene, depending on the relative thermodynamic stability of each product and the activation barrier of hydrogen and methyl shifts, respectively. The residence time of the adsorbate on the lattice is determined by the relative rates of the adsorption and desorption steps, which may be expressed through the simplified Langmuir expression: $r_l/r_T = k_l P(C_nH_m)(1 - \Theta)^n/k_T\Theta^n$ ($n = 1-2$, Θ = fractional surface coverage). From a thermodynamic point of view, adsorption from the gas phase has a negative entropy contribution, and the population of adsorbed alkyl species is therefore expected to decrease with an increasing temperature (e.g., $K_{ads} = k_l/k_T$ decreases). Consequently, one may expect a shorter chain length at higher temperatures, due to a more rapid desorption and subsequent adsorption of a competing molecule.

The propagation step, the rate of which is represented by the rate constant k_p in Scheme 1a, consists of a reaction between the adsorbate and an incoming alkene molecule. The relative rates of the termination and propagation reactions may be expressed as

$$r_p/r_T = k_p P(C_nH_m)/k_T$$

It can be assessed that the activation and conversion pattern of 1-butene over the zeolite catalysts depends on the interaction between the lattice and the alkene, as well as on the concentration of alkenes near the zeolite surface. The former parameter depends on the relative acidic strength of the zeolites considered, while the latter parameter depends on the relative rates of diffusion and reaction within each zeolite under the chosen conditions. According to FTIR adsorption studies, the acidic strengths of our samples are equivalent (see Supporting Information and ref 15). In part b of Scheme 1, the formation of linear and branched oligomers is explicitly taken into account. It can be inferred that as far as the "$O-C_4H_9$" species is concerned, four different structures, having different CH_2/CH_3 ratios (branching), must be considered. The scheme holds for dimers, trimers, etc. For them only a few species are reported for the sake of simplicity.

3.3. Vibrational Spectrum of Gaseous 1-Butene. The gas-phase IR spectrum of 1-butene is reported in the lower part of Figure 1. In general, bands due to vinylic C−H stretching vibrations ($\nu(H_2C{=})$) appear above 3000 cm^{-1}, whereas aliphatic ν(CH) modes are observed below 3000 cm^{-1}. The band observed at 3090 cm^{-1} is thus assigned to $\nu_{asym}(H_2C{=})$ modes, while the $\nu_{sym}(H_2C{=})$ mode is barely visible as a component at about 3015 cm^{-1}. The bands around 2977 cm^{-1} are attributed to the ν(C−H) in the sp^3 hybridized methylene or methyl groups of 1-butene. Resonance effects between CH stretching vibrations and CH deformation overtones complicate the assignments in this region. The absorption centered at 1647 cm^{-1} is assigned to the ν(C=C) stretching mode, and the complex of absorptions between 1500 and 1350 cm^{-1} are due to C−H deformation vibrations (δ(CH)).

SCHEME 1

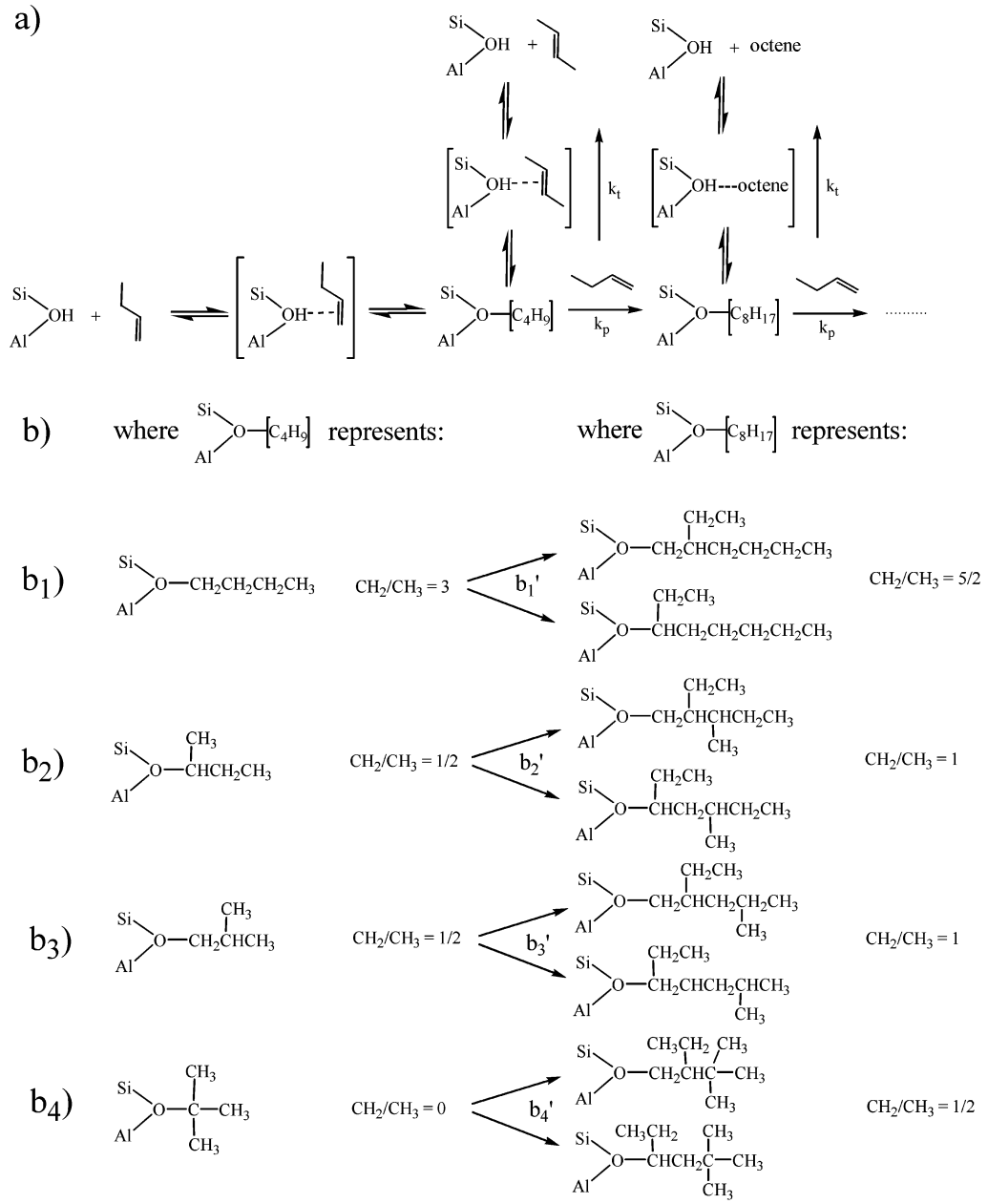

3.4. Vibrational Spectrum of 1-Butene Adsorbed on Zeolite H-Beta at Room Temperature. 1-Butene was adsorbed on the H-beta zeolite at room temperature, and the following spectra are reported in the upper part of Figure 1: the H-beta zeolite previously outgassed at 673 K for 1 h (bold drawn plot), immediately after dosing 5 Torr of 1-butene to the sample (solid drawn plot), and the 1-butene/H-beta system after 3 min of outgassing (dashed plot). Four bands can be seen in the OH stretching region of the pretreated zeolite. The sharp peak at 3746 cm^{-1} is due to the stretching vibrations of weakly acidic Si−OH groups, and the band at 3610 cm^{-1} represents the OH stretching of strongly acidic Brönsted sites.[16] The two further components, observed at 3782 and 3663 cm^{-1}, are ascribed to hydroxyls associated with extra lattice aluminum and/or partially extra lattice aluminum. The assignment of these bands cannot be confidently assessed, owing to the controversial opinion in the literature.[17−19] In any case, both bands are associated with centers having a rather low acidity.

The solid drawn spectrum in the upper part of Figure 1 was collected immediately after dosing 5 Torr 1-butene to the sample at room temperature. The Si−OH band becomes partially eroded (about 30%), while a band located at 3698 cm^{-1} appears. This downward frequency shift of the Si−OH vibrations ($\Delta\nu = -48$) is caused by H-bonding interactions between the instantly formed oligomeric chains and the weakly acidic Si−OH groups. This interpretation is in accord with the observation that saturated hydrocarbons induce the same perturbations when being adsorbed on zeolites.[20,21] The band corresponding to the vibrations of the Brönsted sites appears to be totally consumed upon 1-butene adsorption. The broad and complex absorptions centered at 3490 cm^{-1} arise from Brönsted sites perturbed by the saturated oligomeric chains. Due to the heterogeneity of the Brönsted sites in the H-beta zeolite, several contributions are expected; among them the most prominent component is observed at 3490 cm^{-1} ($\Delta\nu = -120$). The presence of this band implies that the number of formed chains is smaller than the number of Brönsted sites and implicitly that the chains are long. Any traces of gaseous or adsorbed 1-butene cannot be discerned in the spectrum, and the conversion of 1-butene into oligomeric material was obviously complete within a few

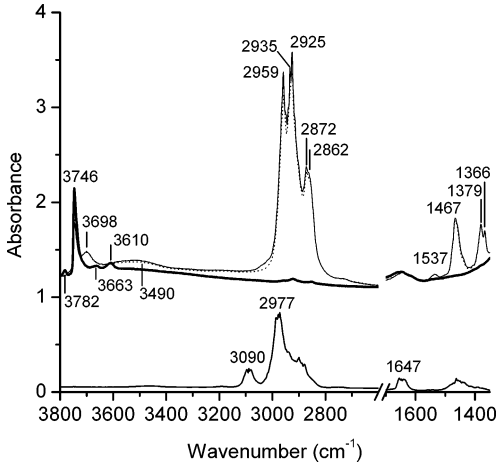

Figure 1. (Upper) FTIR spectra of the H-beta zeolite obtained at 300 K: previously outgassed at 673 K for 1 h (bold drawn plot); immediately after dosing 5 Torr of 1-butene (solid drawn plot); after 3 min of subsequent outgassing (dashed plot). (Lower) FTIR spectrum of gaseous 1-butene.

TABLE 1: Assignments of the IR Bands of 1-Butene and the Oligomers in Zeolite H-Beta

assignment	wavenumber (cm^{-1})
ν(HC═) (1-butene)	3080
$\delta_{\text{in plane}}$(H_2C═) (1-butene)	1416
δ(═CH) (1-butene)	1440
ν_{asym}(CH_3) (1-butene and in oligomers)	2967
ν_{sym}(CH_3) (1-butene and in oligomers)	2875
δ_{asym}(CH_3) (1-butene and in oligomers)	1463
δ (CH_2) (1-butene and in oligomers)	1463
δ_{sym}(CH_3) (1-butene and in oligomers)	1377
ν_{asym}(CH_2) (1-butene and in oligomers)	2934
ν_{sym}(CH_2) (1-butene and in oligomers)	2854
ν_{asym}(CH_2) (in oligomers)	2929
ν_{sym}(CH_2) (in oligomers)	2861
wag (CH) (in oligomers)	1368
ν(C═C) (1-butene on Si−OH groups/Brönsted)	1639/1629

seconds. The asymmetric and symmetric stretching of aliphatic methyl groups are expected to occur in the regions 2975−2950 and 2885−2865 cm^{-1}, respectively.[22,23] The corresponding frequency regions for methylene vibrations are 2940−2915 and 2870−2840 cm^{-1}.[22,23] The bands at 2959 and 2872 cm^{-1} and at 2935/2925 and 2862 (shoulder) cm^{-1} are thus readily assigned to the stretching modes of CH_3 and CH_2 groups, respectively, in the oligomeric chains. The CH bending modes of the oligomers are characterized by a component centered at 1467 cm^{-1} assigned to $\delta_{\text{asym}}(CH_3)$ and $\delta(CH_2)$, a band at 1379 cm^{-1} due to $\delta_{\text{sym}}(CH_3)$, and a component at 1366 cm^{-1}, which is probably associated with a wagging mode of CH_2 groups. The weak component at 1537 cm^{-1} can tentatively be ascribed to allylic cationic species arising from dehydrogenation of the oligomers.[15] The assignments of 1-butene and the formed oligomers in the beta zeolite are summarized in Table 1.

Upon 3 min of outgassing (dashed plot), the spectrum of the beta zeolite with the oligomeric material remains virtually unchanged, showing that the contribution from the gas phase is negligible and that the oligomeric material is trapped within the zeolite pores.

The results show that, when 1-butene is adsorbed at room temperature, the zeolite is immediately filled with oligomeric material. From the relative intensity I of the stretching modes of CH_3 (band at 2959 cm^{-1}) and of CH_2 (band at 2925 cm^{-1}) it is possible to withdraw some information about the oligomeric structure. The extinction coefficient of the $\nu(CH_3)$ and $\nu(CH_2)$ modes of saturated hydrocarbons can be obtained by measurements on standards. (We have measured n-heptane in CCl_4 and recorded six spectra in a cell with variable thickness. The resulting extinction coefficient for CH_3 was 4.843×10^5 cm^2/mol and 2.291×10^5 cm^2/mol for CH_2.) From such measurements we can deduce that the $\epsilon CH_3/\epsilon CH_2$ is about 2.2. In 1-butene, the CH_3/CH_2 ratio is 1:1, and accordingly the intensity ratio $I(CH_3)/I(CH_2)$ is expected to be close to 2:1. When the chains grow, the number of CH_3 remains constant, whereas the number of CH_2 increases by one for each monomer that adds to the chain (if we consider the formation of a linear chain, as reported in Scheme 1b). Experimentally, we observe a nearly equivalent intensity of the components at 2959 and at 2925 cm^{-1} (i.e., $I(CH_3) \approx I(CH_2)$), and the ratio between CH_2 and CH_3 groups in the oligomeric chains should be around 2. This suggests that, in the beta zeolite, the oligomerization reaction follows paths b_1 and b_2 as reported in Scheme 1 and is not accompanied by substantial branching. This conclusion is in agreement with the general considerations that have been advanced before.[24] The results furthermore suggest that the chains have grown extensively.

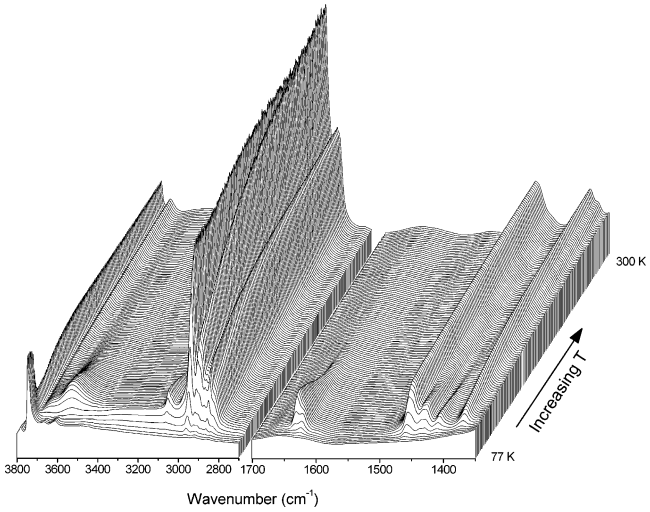

Figure 2. Overview: FTIR spectra of H-beta and 1-butene (adsorbed at 77 K) in the temperature range 77−300 K.

Details around the initial stages of the reaction and the subsequent chain growth cannot be extracted from this experiment due to the high reactivity of 1-butene in the system. To suppress the reaction rates and to follow each step of the reactions on a more detailed level, it was decided to adsorb 1-butene on the zeolite at 77 K.

3.5. 1-Butene Adsorbed on H-Beta at Low Temperature. Temperature-resolved IR spectroscopy has previously proved to give detailed information on the precursor formation and the different stages of propene oligomerization in H-mordenite.[20] Compared to propene, 1-butene is expected to oligomerize at an even higher rate, and reducing the sample temperature appeared to be necessary to follow the reaction by IR spectroscopy. Thus, a similar approach was adopted in this study, and 1-butene was adsorbed on the zeolites while being kept at liquid nitrogen temperature. The IR cell was subsequently equilibrated thermally with the surroundings while spectra were collected continuously every 5.4 s.

3.5.1. General Overview of the 1-Butene/H-Beta System. Figure 2 gives an overview of the whole set of spectra collected in the temperature range 77−300 K for the H-beta zeolite. The bands belonging to the pretreated zeolite were described in section 3.4. The initial interaction between the Brönsted acidic

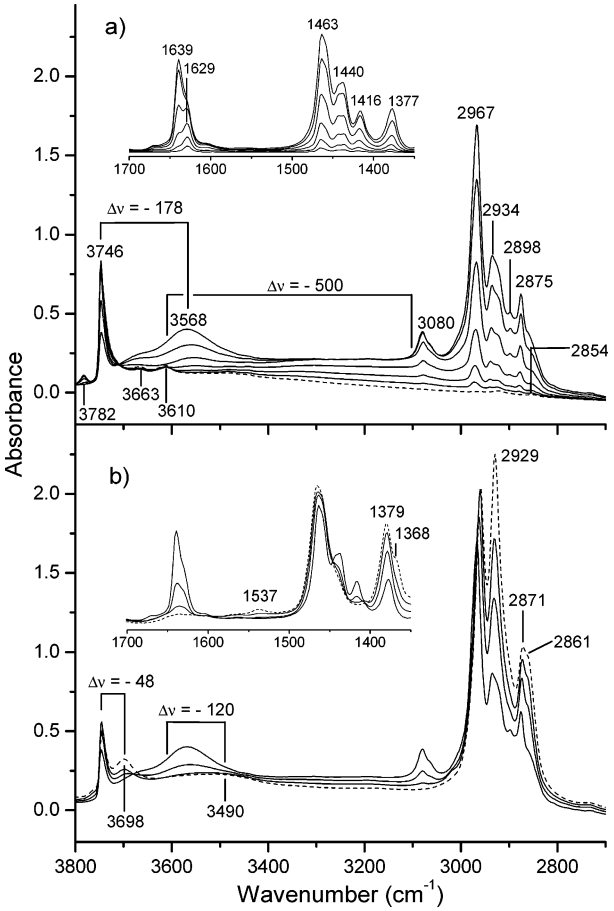

Figure 3. Selected FTIR spectra of H-beta and 1-butene (adsorbed at 77 K) from Figure 2. (a) Temperature range where adduct formation takes place. (b) Temperature range where oligomerization dominates. The spectral regions between 1700 and 1350 cm^{-1} are background subtracted and shown as insets.

sites and the π-electrons of the reactant is testified by the growth of the broad absorption between 3500 and 2900 cm^{-1} that characterizes the first few spectra. This absorption results from the perturbed ν(OH) vibrations of the adduct. By further increase of the temperature and thereby the partial pressure of 1-butene, an analogous perturbation of the weakly acidic Si−OH groups results in the appearance of a band at 3568 cm^{-1} ($\Delta\nu = -178$). The bands at 3080 and around 1630 cm^{-1} confirm that 1-butene is present in the system as the H-bonded adduct at the lower temperatures. Contrary to the experiment performed at room temperature, 1-butene is not consumed immediately by oligomerization at this temperature. The concentration of the adducts reaches a maximum, then readily levels off and starts to decline. At the same time, oligomeric chains are formed, as evidenced by the intensity increase in the prominent oligomer bands around 2930 and 2875 cm^{-1}. To evaluate the results in a more detailed manner, the whole series of spectra has been divided into two parts: the adduct formation and the oligomerization, represented by Figures 3a and 3b, respectively. Figure 3a gives the first few spectra collected until the temperature where the concentration of the H-bonded precursor reaches its maximum. Figure 3b presents some selected spectra from the temperature interval between the highest adduct concentration and 300 K.

3.5.2. Formation of the H-Bonded Precursors. In Figure 3a, the first collected spectrum, i.e., that of the pretreated zeolite, is represented by the dash drawn plot. The region 1700−1350 cm^{-1} is shown as a difference in an inset. The previously mentioned interaction between the weakly acidic Si−OH groups and 1-butene is evidenced by the erosion of the band at 3746 cm^{-1} with a parallel growth of the band at 3568 cm^{-1} ($\Delta\nu = -178$) when 1-butene starts to vaporize and reaches the sample. An isobestic point, confirming this correlation, can be seen at 3709 cm^{-1}. In a similar manner, the Brönsted sites are consumed and create the broad absorption extending from 3500 cm^{-1} (with a maximum centered at 3100 cm^{-1}, $\Delta\nu \approx -500$) as they interact with 1-butene and form the H-bonded adduct. The band at 3080 cm^{-1} represents the vinylic CH vibrational modes of 1-butene. The absorptions at 2967 and 2875 cm^{-1} are attributed to $\nu_{asym}(CH_3)$ and $\nu_{sym}(CH_3)$ vibrations, respectively. The bands at 2934 and 2854 cm^{-1} are ascribed to the corresponding $\nu(CH_2)$ modes. The intensity ratio of the two doublets is about 2, as expected from the CH_3/CH_2 ratio in 1-butene. The 2934 cm^{-1} band has a shoulder on its low-frequency side that most likely represents methylene groups in the oligomeric chains (vide ultra).

The band representing the ν(C═C) modes of 1-butene consists of two components, one at 1639 cm^{-1} and another at 1629 cm^{-1}. The 1639 cm^{-1} band is assigned to 1-butene weakly adsorbed on Si−OH groups, whereas the 1629 cm^{-1} band represents stronger perturbed 1-butene adsorbed on Brönsted sites. The corresponding vibration of gaseous 1-butene absorbs at 1647 cm^{-1} (Figure 1). Previous observations made for several other adducts isolated in protonic zeolites show a reduction of the gas-phase C═C stretching frequency of 15−20 cm^{-1} due to the weakening of the bond induced by the interaction with the Brönsted protons.[25] The relative intensities of the two ν(C═C) bands change at increasing 1-butene coverage. At the lower coverages, the olefin preferentially occupies the strongly acidic Brönsted sites of the zeolite, while the interaction with the weaker acidic Si−OH groups becomes more prominent at higher 1-butene loadings. Spectra obtained in the presence of higher 1-butene loadings show the appearance of two components at 1670 and 1604 cm^{-1} that we ascribe to the P and Q branches of a gaseous-like fraction of 1-butene with some restricted rotation.

The bands in the range 1500−1350 cm^{-1} have been assigned as follows: the complex absorption centered at 1463 cm^{-1}, $\delta_{asym}(CH_3)$ and $\delta(CH_2)$ in 1-butene and in oligomeric chains; complex absorption centered at 1440 cm^{-1}, δ(═C−H) in 1-butene; 1416 cm^{-1}, $\delta_{in\ plane}(H_2C═)$ in 1-butene; 1377 cm^{-1}, $\delta_{sym}(CH_3)$ in 1-butene and in the oligomers.

3.5.3. Oligomerization of Adsorbed 1-Butene. Figure 3b covers the temperature region where oligomerization of 1-butene is the dominant reaction. The last collected spectrum (300 K) is reported as a dashed plot. When 1-butene is consumed, as evidenced by the decrease in the bands at 3080 and 1639 cm^{-1}, the absorption at 3746 cm^{-1}, representing the Si−OH groups, becomes partially restored, and the band at 3568 cm^{-1} decreases. However, as saturated chains now are filling the channels and thus interact with the acidic sites of the zeolite, a part of the Si−OH groups is not regained, but is weakly perturbed to give a band at 3698 cm^{-1} ($\Delta\nu = -48$). This band increases in intensity as the oligomers grow. Much the same features can be seen for the Brönsted sites: The broad absorption that extends from 3500 cm^{-1} declines, while a new absorption centered at 3490 cm^{-1} ($\Delta\nu = -120$), representing the weaker interaction with the saturated oligomers, appears.

The relative intensities of the bands in the CH_2/CH_3 stretching region change markedly during the chain propagation. The band at 2967 cm^{-1}, representing methyl groups, reaches a level that remains nearly constant throughout the experiment (more clearly illustrated by Figure 2). Among the bands associated with

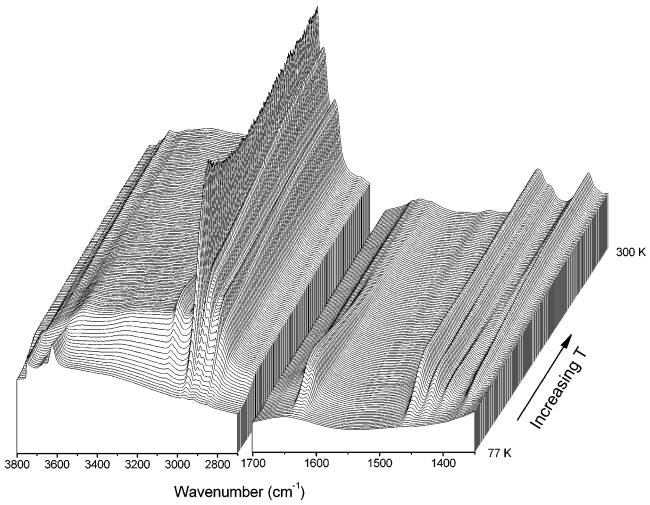

Figure 4. Overview: FTIR spectra of H-MCM-22 and 1-butene (adsorbed at 77 K) in the temperature range 77−300 K.

bending modes, the component at 1463 cm^{-1}, representing the $\delta_{asym}(CH_3)$ modes, behaves the same way. The behavior of these bands, i.e., the fact that they are barely affected by the chain growth, is predicted by the oligomerization mechanism b1 and b2 given in Scheme 1. According to mechanism b2, when all the 1-butene is adsorbed on the zeolite, the bands representing the methyl groups will remain constant, as additional methyl groups are not generated during the oligomerization. On the contrary, the number of methylene groups will increase as the oligomers are growing, and the corresponding bands are expected to grow accordingly and gradually approach an $I(CH_3)/I(CH_2)$ ratio close to 1. The 2934 cm^{-1} band of Figure 3a, representing the CH_2 vibrations, predominantly of 1-butene, is red-shifted to 2929 cm^{-1} in the last collected spectrum in Figure 3b. This agrees well with the assignment of the low-frequency shoulder of the 2934 cm^{-1} band (Figure 3a) to oligomeric $\nu(CH_2)$ vibrations. The number of CH groups is also expected to increase as a result of a linear oligomerization. Unfortunately, the IR intensity of CH modes is very modest and also mixed with the other groups. The changes seen in the 1500−1350 cm^{-1} region due to chain propagation are dominated by the nearly total disappearance of the 1440 and 1416 cm^{-1} bands. These components were previously assigned to the $\delta(=C-H)$ and $\delta_{in\ plane}(H_2-C=)$ modes of 1-butene. In addition, a shoulder appears at 1368 cm^{-1}. This shoulder can be associated with the wagging mode of the growing chains.

The final $I(CH_3)/I(CH_2)$ ratio in this experiment is similar to that observed in the 300 K experiment. This result indicates that the adducts are very stable in the temperature range studied and that the accessibility of monomers is not rate-limiting for the oligomerization reaction at either temperature. This result suggests that the oligomerization reaction is not diffusion-limited in the H-beta zeolite at temperatures up to 300 K.

3.6. 1-Butene Adsorbed on H-MCM-22 at 77 K. A parallel experiment where 1-butene was adsorbed at 77 K was carried out for H-MCM-22. The results will be presented similarly to those in the preceding section. Figure 4 gives an overview of the whole set of spectra collected in the temperature range 77−300 K. Figure 5a reports the spectra collected until the temperature where the concentration of the H-bonded precursor reaches its maximum. Figure 5b presents some selected spectra from the temperature interval between the highest adduct concentration and 300 K.

The IR spectrum in the OH stretching region of H-MCM-22 (Figures 4 and 5a) shows many components as already described

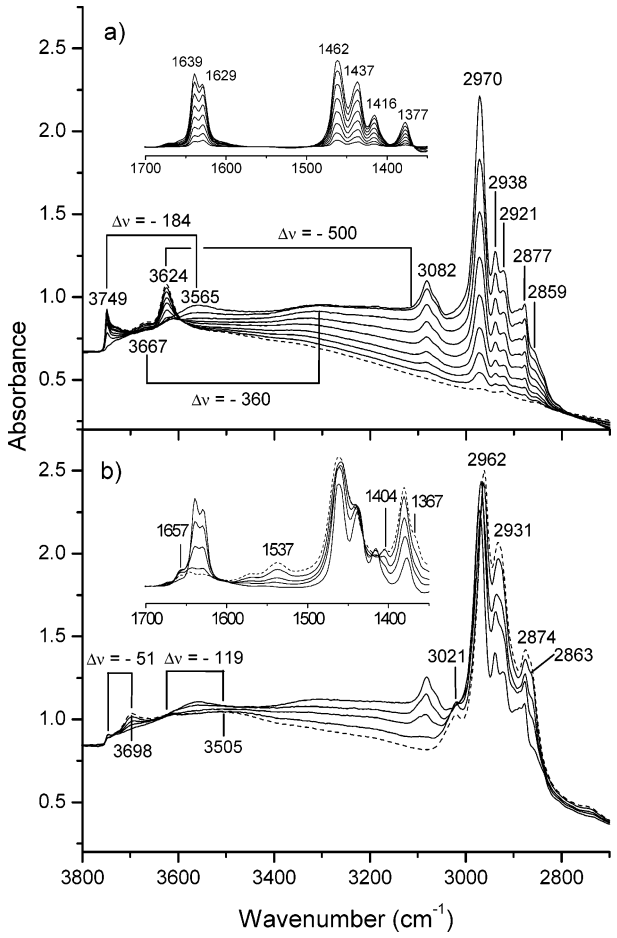

Figure 5. Selected FTIR spectra of H-MCM-22 and 1-butene (adsorbed at 77 K) from Figure 4. (a) Temperature range where adduct formation takes place. (b) Temperature range where oligomerization dominates. The spectral regions between 1700 and 1350 cm^{-1} are background subtracted and shown as insets.

by Onida et al.:[15,26] (i) isolated Si−OH groups absorbing at 3749 cm^{-1}, (ii) a shoulder at about 3730 cm^{-1} due to internal Si−OH groups; (iii) a weak absorption at 3667 cm^{-1} related to Al−OH species partially anchored to the zeolitic framework (a product of incipient dealumination); (iv) a band at 3624 cm^{-1} (for which two components have been singled out) due to Si(OH)Al species located in the 10-ring channels and in the super cages; (v) a shoulder at about 3580 cm^{-1} attributed to Si(OH)Al species located in strongly constrained environment, probably in the hexagonal prism capping the super cages.

Generally speaking, the 1-butene/H-MCM-22 system behaves similar to what has been observed for 1-butene/H-beta. Some differences can, however, be pointed out (see section 3.6.2). Also in this case, the initial adduct formation is evident and the subsequent decline in the adduct concentration is accompanied by the oligomerization as shown in Figure 4. A relatively prominent difference from the beta zeolite appears to be the higher temperature required for MCM-22 to reach the maximum adduct concentration. Since adduct formation is thermodynamically favored at low temperatures ($\Delta S < 0$), this difference must be kinetically controlled, either by a slower adduct formation reaction or by a slower onset of the adduct conversion reaction. H-bonding is normally not an activated process, and the Arrhenius factor is expected to be similar for the various zeolite/1-butene systems at comparable temperatures. Therefore, a slower adduct formation is probably associated with a lower olefin concentration in the vicinity of the active sites.

The adduct conversion reaction is likely to be an activated process, and it is difficult to determine from this observation alone whether the first or second reaction step is responsible for the observed difference between the H-beta and MCM-22 catalysts. This will be discussed in more detail below.

3.6.1. Formation of the H-Bonded Precursors. The dashed curve in Figure 5a represents the pretreated zeolite. The H-bonded precursor is also in this case evidenced by a complete consumption of the Brönsted sites accompanied by a broad and complex absorption extending between 3500 and 2800 cm^{-1}: Two maxima at about 3300 and 3100 cm^{-1} can be distinguished for this absorption, confirming the heterogeneity of the strong Brönsted sites. Downward shifts of about 360 cm^{-1} and approximately 500 cm^{-1} with respect to the free OH groups can be observed. The analogous interaction between the Si−OH groups and 1-butene creates a band with a maximum around 3565 cm^{-1} ($\Delta\nu = -184$ cm^{-1}). We observe that, in contrast to what was found for the beta zeolite, the formation of adducts with Si−OH groups starts at first stages and proceeds until the Si−OH groups eroded completely. This implies that in the case of MCM-22 the reactivity of the Si−OH groups saturating mouth channels is readily involved in H-bonding interaction with 1-butene. The final spectrum of Figure 5a is characterized by an absorption continuum where components associated with sites with strong acidic character are hardly distinguishable from those related to less acidic sites.

The vinylic CH vibrational modes can be observed in Figure 5a at 3082 cm^{-1}. In the CH_2/CH_3 stretching region the absorptions at 2970 and 2877 cm^{-1} are attributed to $\nu_{asym}(CH_3)$ and $\nu_{sym}(CH_3)$ vibrations, respectively. The 2938 cm^{-1} band is assigned to $\nu_{asym}(CH_2)$ of 1-butene, and the corresponding frequency of the oligomers is located at 2921 cm^{-1}. The latter assignment is verified by Figure 5b, which shows that the 2921 cm^{-1} band increases in intensity relative to the 2938 cm^{-1} band when the temperature is increased. The shoulder at 2859 cm^{-1} represents $\nu_{sym}(CH_2)$ modes. In the frequency region 1700−1350 cm^{-1}, the frequencies are nearly identical to those seen for the beta zeolite (3.5.2), and the assignments are thus the same. However it should be noticed that the ratio between the 1639 and 1629 cm^{-1} bands (i.e., the ratio between weakly and strongly adsorbed 1-butene) is different from the case of the beta zeolite. This feature suggests that the number of sites able to give a strong interaction with 1-butene is less abundant than in the case of beta zeolite. Also in this case, for higher 1-butene loadings, two components ascribable to a hindered rotator are visible at about 1670 and 1604 cm^{-1}.

3.6.2. Oligomerization of Adsorbed 1-Butene. The evolution of the spectra reported in Figure 5b shows some important changes in the OH stretching region. In particular, we observe the growth of bands at 3698 and 3505 cm^{-1}, suggesting that both silanol and Brönsted groups become perturbed by saturated hydrocarbons when the oligomers are formed. A parallel decrease of absorbance in the range 3500−2800 cm^{-1} indicates a decreasing number of olefinic monomers involved in strong H-bonds. The consumption of 1-butene is verified by the decreasing intensity of the band at 3082 cm^{-1}. The parallel growth of bands at 3021 and 1657 cm^{-1} (not observed for the beta zeolite) suggests the formation of *trans*-2-butene via a branched intermediate $O-CH_2(CH_3)-CH_2-CH_3$. The $\nu(H_2C=)$ and $\nu(C=C)$ vibrational modes of *trans*-2-butene in H-ZSM-5 have previously been reported to absorb at 3022 and 1657 cm^{-1}. The formed *trans*-2-butene molecules are not subjected to oligomerization and can even be seen in the last spectrum (300 K). The apparent lack of reactivity of these molecules might be due to steric constraints imposed on the highly branched oligomers that will form from *trans*-2-butene. Similar features are expected also for termination products derived from oligomerization steps higher than the first (i.e., octenes). These species together with unreacted butenes form H-bonded adducts with Brönsted sites, as documented by the persisting broad absorption in the range 3500−2800 cm^{-1}. During the oligomerization, the band at 2970 cm^{-1} in Figure 5a is red-shifted to 2962 cm^{-1}, as shown by the last spectrum of Figure 5b. This was not observed for the beta zeolite. The bands at 2938 and 2921 in Figure 5a merge together in a band that ends up at 2931 cm^{-1} in Figure 5b. This is also the case for the 2877 and 2859 cm^{-1} bands of Figure 5a, which end up at 2874 cm^{-1} in the last spectrum of Figure 5b. The relative intensities of the bands corresponding to CH_3 and CH_2 groups reveal that the average oligomer chain length is significantly shorter in MCM-22 compared to the beta zeolite. In the 1700−1500 cm^{-1} range, the main features of the last spectrum collected at room temperature are the following: a component at 1657 cm^{-1} (due to olefinic species); two components at 1639 and 1629 cm^{-1} (residual presence of 1-butene); and a small component at 1537 cm^{-1}, interpreted to represent allylic cationic species.[15] The CH bending region reported in Figure 5b shows some peculiar behaviors. In particular, we observe that the components at 1437 and 1416 cm^{-1} are only partially consumed, in agreement with the presence of alkenes (such as 2-butene). Furthermore the growth of a component at 1404 cm^{-1} can be associated with symmetric bending modes of CH_3 species in branched oligomers.

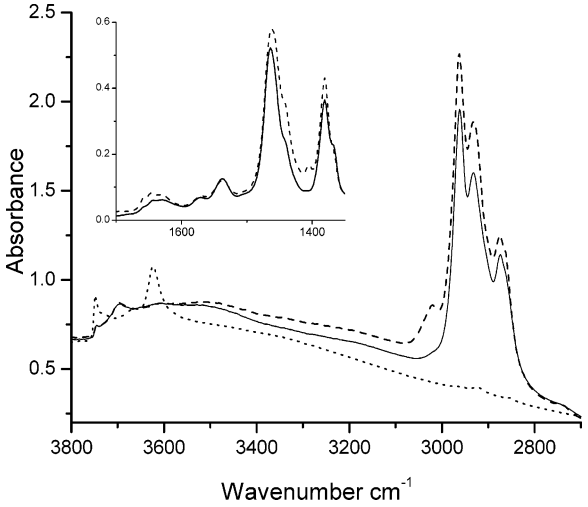

Figure 6. Effect of outgassing the H-MCM-22/1-butene system at room temperature. The dotted curve represents the background, the dashed curve is the last spectrum of Figure 5b, and the solid drawn curve shows the effect of 10 min of outgassing at room temperature.

To identify components related to weakly bonded species, the sample was outgassed for 10 min at room temperature. The following spectra are shown in Figure 6: H-MCM-22 after pretreatment (dotted plot); H-MCM-22 after adsorption of 1-butene and heating to room temperature (dashed plot); after an additional outgassing for 10 min (solid drawn spectrum). The background-subtracted CH bending region is represented by the inset. A clear decrease in the intensity of the bands at 2962, 2931, 2874, 1461, and 1437 cm^{-1}, due to olefinic (ν and δ modes of (CH_2) and (CH_3) groups) species, can be observed. Furthermore, a strong erosion of the components at 3021 and 1404 cm^{-1}, associated with ν and δ modes of (CH) groups in alkenes, can be seen. The broad absorption in the 3500−2800 cm^{-1} range associated with Brönsted sites involved in strong

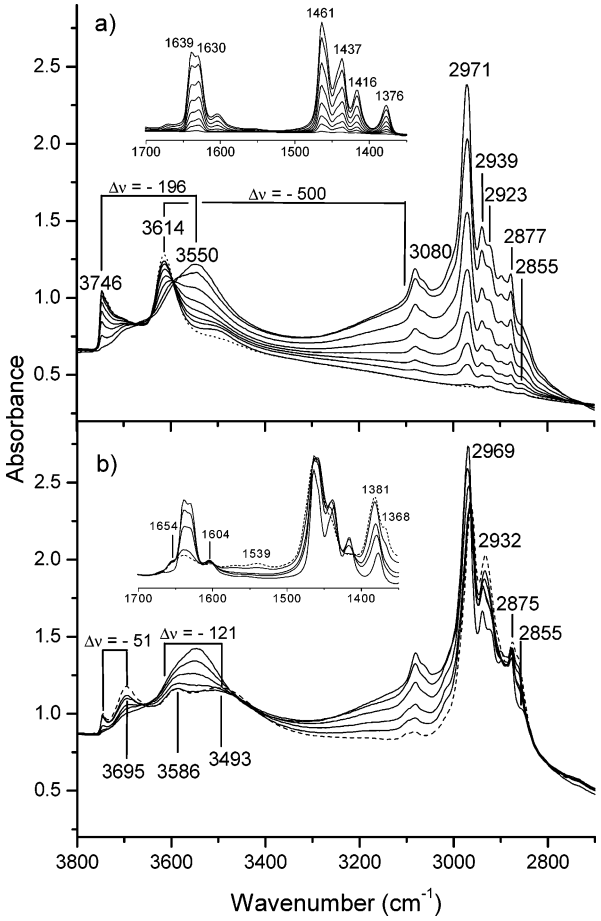

Figure 7. Selected FTIR spectra of H-mordenite and 1-butene (adsorbed at 77 K). (a) Temperature range where adduct formation takes place. (b) Temperature range where oligomerization dominates. The spectral regions between 1700 and 1350 cm^{-1} are background subtracted and shown as insets.

H-bonds is also clearly reduced. The components of the original spectrum in the hydroxyl stretching region are not restored upon outgassing, not even the Si−OH groups. This final observation suggests a high density of oligomeric chains growing close to the channel mouths and perturbing Si−OH groups present on external surfaces. The observation of *trans*-2-butene formation in MCM-22 as well as the shorter overall chain length in this catalyst compared to H-beta both point to a decrease in the r_P/r_T ratio in MCM-22 compared to H-beta. As discussed above, this decrease can be related to the rate constants, but also to the concentration of monomers in the vicinity of the active sites. This observation in addition to the slower accumulation of the adducts in the MCM-22 catalyst (see above) indicates that the oligomerization reaction is diffusion-limited over MCM-22. This conclusion is in agreement with the smaller pore dimensions in MCM-22 compared to the beta zeolite.

3.7. 1-Butene Adsorbed on H-Mordenite at 77 K. The details of the experiment for the mordenite sample are represented by Figures 7 and 8. This experiment does not introduce any new striking features, but it is included for the sake of completeness. The overview of the entire set of spectra is in this case left out.

3.7.1. Formation of the H-Bonded Precursors. The spectrum of the pretreated zeolite is presented as a dashed plot in Figure 7a. It is generally agreed that the 3746 cm^{-1} band corresponds to the OH stretch of terminal Si−OH groups located mainly on external surfaces. A component at about 3730 cm^{-1} (observed as a shoulder) is ascribed to Si−OH groups mainly

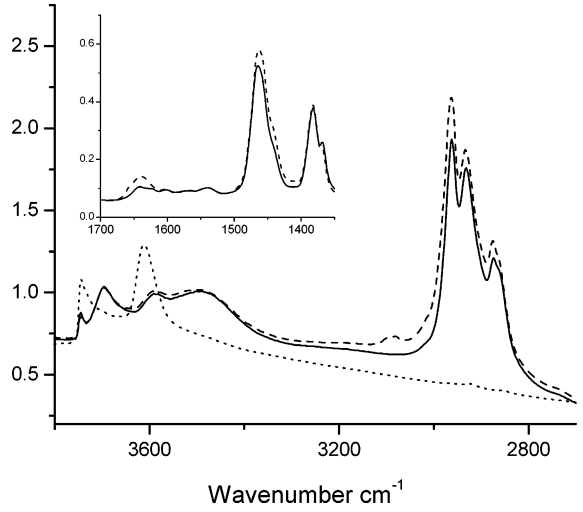

Figure 8. Effect of outgassing the H-mordenite/1-butene system at room temperature. The dotted curve represents the background, the dashed curve is the last spectrum of Figure 7b, and the solid drawn curve shows the effect of 10 min of outgassing at room temperature.

located on internal defects. The band representing the Brönsted groups is very broad, and it was previously described as a complex band consisting of at least two components, one centered at 3614 cm^{-1} and the other at a lower frequency (around 3585 cm^{-1}) respectively assigned to hydroxyls vibrating in the 12-ring main channels and those present in the smaller eight-ring channels.[27]

Upon 1-butene adsorption, the perturbations of the OH groups are much the same as already seen for H-MCM-22. The 3550 cm^{-1} band and the broad absorption extending from 3400 cm^{-1} in Figure 7a are the obvious results of perturbation of silanol ($\Delta\nu = -196$ cm^{-1}) and Brönsted groups ($\Delta\nu \approx -500$ cm^{-1}). It should be noticed that in the case of mordenite strong acidic sites form a band that is distinct from the component associated with adducts formed with Si−OH groups. The bands of adsorbed 1-butene in the temperature interval represented by Figure 7a do not add much to the results from the previous sections. All the bands appear to reproduce very well the frequencies of 1-butene in H-MCM-22. Superimposed on the contribution of P and Q branches of gaseous-like fractions, a band at 1604 cm^{-1}, attributed to extraordinary strong C═C bonds, appears. The responsible species could be isobutene, for which the inductive effect of the methyl groups increases the basicity of the π electrons.

3.7.2. Oligomerization of Adsorbed 1-Butene. It can be seen from Figure 7b that a part of the Si−OH band (3746 cm^{-1}) is restored when 1-butene is consumed by the oligomerization reactions. Most of the remaining Si−OH groups are perturbed by the saturated chains, giving the band at 3695 cm^{-1} ($\Delta\nu = -51$ cm^{-1}). The broad absorption corresponding to the interaction between 1-butene and the Brönsted sites also declines. At the same time the Brönsted sites become perturbed by the oligomeric chains and create the band at 3493 cm^{-1} ($\Delta\nu = -121$ cm^{-1}). The last spectrum, reported as a dashed plot, shows clearly the component at 3586 cm^{-1} due to unperturbed Brönsted sites. This confirms the previous assignment of this band to sites located in the eight-ring channels, a position where 1-butene is too bulky to access. In the 1700−1350 cm^{-1} range, the main features of the last collected spectrum have a very close resemblance to the spectra observed for H-beta and H-MCM-22 and were thus discussed in sections 3.5.3 and 3.6.2.

To identify the components related to weakly bonded species still being present at 300 K, the sample was finally outgassed

for 10 min also in this case. The following spectra are shown in Figure 8: H-mordenite after pretreatment (dotted plot); H-mordenite after adsorption of 1-butene and heating to room temperature (dashed plot); after an additional outgassing for 10 min (solid drawn spectrum). The background-subtracted CH bending region is represented by the inset. Similar to what we reported for H-MCM-22, a decrease in the intensity of the bands at 2969, 2932, 2875, 1461, and 1437 cm^{-1}, due to olefinic (ν and δ modes of (CH_2) and (CH_3) groups) species, can be observed. Furthermore, a strong erosion of the component at 3080 cm^{-1}, associated with vinylic CH modes in 1-butene, can be seen. The broad absorption in the 3500−2800 cm^{-1} range associated with Brönsted sites involved in strong H-bonds is also lowered. The components of the original spectrum in the hydroxyl stretching region are not restored upon outgassing.

4. Conclusions

FTIR proved to be a well-suited technique to gain insight into the mechanistic aspects of 1-butene oligomerization in zeolites. When 1-butene was adsorbed on the samples at room temperature, the oligomerization occurred instantly. By adsorbing 1-butene on the samples at liquid nitrogen temperature and subsequently allowing the IR cell to equilibrate thermally with the surroundings, the different stages of the reaction could be followed. 1-Butene forms H-bonded adducts, both with the weakly acidic silanol groups and the strongly acidic Brönsted sites. The double bond of 1-butene was accordingly perturbed weakly by interaction with the silanol groups and strongly by interaction with the Brönsted sites. These adducts were stable only at the lowest temperatures. The red shifts observed for the strong Brönsted sites are similar in all three materials ($\Delta\nu = -500$ cm^{-1}), suggesting a rather equal acidity of the involved sites. The adduct concentration soon reached a maximum when the temperature was increased and vanished as they reacted further to oligomers. It was furthermore observed that the adducts accumulated fastest over H-beta. This is indicative of diffusion-limited oligomerization reactions over MCM-22 and mordenite and agrees well with the smaller pore dimensions in MCM-22 and mordenite. When starting the experiment with the beta zeolite at 77 K, the final CH_3/CH_2 ratio was similar to that observed when the starting temperature was 300 K. This result also supports that the accessibility of monomers is not rate-limiting for the oligomerization reaction in the beta zeolite and that the oligomerization reaction is not diffusion-limited at temperatures up to 300 K.

The lengths of the oligomeric chains turned out to be dependent on the zeolite topology. Among these investigated samples, the chains grow most extensively in the three-dimensional beta zeolite. The mechanistic observations made are in agreement with the mechanism given in Scheme 1b.

Acknowledgment. M.B. is grateful for financial support from the VISTA program of Statoil and the Marie Curie Foundation. S.B. acknowledges INSTM Consortium for financial support from the 2002 PRISMA project.

Supporting Information Available: Acidity of H-beta, H-MCM-22, and H-mordenite probed by CO and FTIR at 77 K. This material is available free of charge via the Internet at http://pubs.acs.org.

References and Notes

(1) Ipatieff, V. N.; Egloff, G. *Oil Gas J.* **1934**, *33*, 31.
(2) Ipatieff, V. N. *J. Ind. Eng. Chem.* **1935**, *27*, 1067−1069.
(3) Ipatieff, V. N.; Corson, B. B. *J. Ind. Eng. Chem.* **1935**, *27*, 1069−1071.
(4) Ipatieff, V. N.; Corson, B. B.; Egloff, G. *J. Ind. Eng. Chem.* **1935**, *27*, 1077−1081.
(5) Ipatieff, V. N.; Pines, H. *J. Ind. Eng. Chem.* **1935**, *27*, 1364−1369.
(6) Wasserscheid, P.; Eichmann, M. *Catal. Today* **2001**, *66*, 309−316.
(7) Sohn, J. R. *Catal. Today* **2002**, *73*, 197−200.
(8) Golombok, M.; de Bruijn, J. *Ind. Eng. Chem. Res.* **2000**, *39*, 267−172.
(9) Güray, I.; Warzywoda, J.; Bac, N.; Sacco, A. *Microporous Mesoporous Mater.* **1999**, *31*, 241−251.
(10) Higgins, J. B.; LaPierre, R. B.; Schlenker, J. L.; Rohrman, A. C.; Wood, J. D.; Kerr, G. T.; Rohrbaugh, W. J. *Zeolites* **1988**, *8*, 446−452.
(11) Newsam, J. M.; Treacy, M. M. J.; Koetsier, W. T.; Gruyter, C. B. *Proc. R. Soc. London A* **1988**, *420*, 375−405.
(12) Baerlocher, C.; Meier, W. M.; Olson, D. H. *Atlas of Zeolite Structure Types*, 5th ed.; Elsevier: New York, 2001.
(13) Souverijns, W.; Verrelst, W.; Vanbutsele, G.; Martens, J. A.; Jacobs, P. A. *J. Chem. Soc., Chem. Commun.* **1994**, 1671−1672.
(14) Lawton, L.; Leonowicz, M. E.; Partridge, R. D.; Chu, P.; Rubin, M. K. *Microporous Mesoporous Mater.* **1998**, *23*, 109−117.
(15) Onida, B.; Geobaldo, F.; Testa, F.; Aiello, R.; Garrone, E. *J. Phys. Chem. B* **2002**, *106*, 1684−1690.
(16) Bordiga, S.; Roggero, I.; Ugliengo, P.; Zecchina, A.; Bolis, V.; Artioli, G.; Buzzoni, R.; Marra, G. L.; Rivetti, F.; Spanò, G.; Lamberti, C. *J. Chem. Soc., Dalton Trans.* **2000**, *21*, 3921−3929.
(17) Pazè, C.; Bordiga, S.; Lamberti, C.; Salvalaggio, M.; Zecchina, A.; Bellussi, G. *J. Phys. Chem. B* **1997**, *101*, 4740−4751.
(18) Kiricsi, I.; Flego, C.; Pazzuconi, G.; Parker, W.; Millini, R.; Perego, C.; Bellussi, G. *J. Phys. Chem.* **1994**, *98*, 4627−4630.
(19) Zecchina, A.; Bordiga, S.; Spoto, G.; Scarano, Petrini, G.; Leofanti, G.; Padovan, M. *J. Chem. Soc., Faraday Trans.* **1992**, *88*, 2959−2969.
(20) Geobaldo, F.; Spoto, G.; Bordiga, S.; Lamberti, C.; Zecchina, A. *J. Chem. Soc., Faraday Trans.* **1997**, *93*, 1243−1249.
(21) Spoto, G.; Bordiga, S.; Ricchiardi, G.; Scarano, D.; Zecchina, A.; Borello, E. *J. Chem. Soc., Faraday Trans.* **1994**, *90*, 2827−2835.
(22) Socrates, G. *Infrared and Raman Characteristic Group Frequencies, Tables and Charts*; John Wiley and Sons Ltd.: West Sussex, 2001.
(23) Colthup, N. B.; Daly, L. H.; Wiberley, S. E. *Introduction to Infrared and Raman Spectroscopy*; Academic Press: New York, 1975.
(24) Knifton, J. F.; Sanderson, J. R. *Catal. Lett.* **1994**, *28*, 223−230.
(25) Pazè, C.; Sazak, B.; Zecchina, A.; Dwyer, J. *J. Phys. Chem. B* **1999**, *103*, 9978−9986
(26) Onida, B.; Geobaldo, F.; Testa, F.; Crea, F.; Garrone, E. *Microporous Mesoporous Mater.* **1999**, *30*, 119−127.
(27) Bordiga, S.; Lamberti, C.; Geobaldo, F.; Zecchina, A.; Turnes Palomino, G.; Otero Areán, C. *Langmuir* **1995**, *11*, 527−533.